A Study on the Properties of Sodium Dodecyl Sulfate Surfactant-Assisted Zinc Oxide Thin Films Doped with Molybdenum

Agnes C. Nkele [1, 2]
https://orcid.org/0000-0003-4574-2123
chinecherem.nkele@unn.edu.ng

David C. Okeudo [1]
https://orcid.org/0009-0003-6100-7978

B. C. N. Obitte [1]
https://orcid.org/0000-0001-5785-892X

Fabian I. Ezema [1, 3, 4, 5]
https://orcid.org/0000-0002-4633-1417

Abstract

In this article, we focused on studying the characteristics of sodium dodecyl sulfate-assisted zinc oxide materials synthesised using molybdenum as a dopant at varying concentrations of 0 M, 0.3 M and 0.5 M. The structural, morphological, elemental and optical characterisations of the synthesised films were studied using scanning electron microscopy, X-ray diffractometry, energy dispersive X-ray spectroscopy, and an ultraviolet-visible spectrophotometer. Nanorod morphology yielded a hexagonal wurtzite structure from the morphological and structural results. Plots from energy dispersive X-rays confirmed the presence of basic elemental constituents: zinc, oxygen and molybdenum. The optical results gave high absorbance and reduced reflectance trends for the doped samples towards lower wavelength regions. The undoped, 0.3 M and 0.5 M molybdenum-doped zinc oxide films recorded energy band gap values of 3.70 eV, 3.84 eV and 3.97 eV respectively. The prepared zinc oxide films would be useful in solar cell and optoelectronic devices.

Keywords: zinc oxide, surfactant, sodium dodecyl sulfate, molybdenum, doping, energy band gap

1 Department of Physics and Astronomy, University of Nigeria.
2 Department of Physics, Colorado State University, United States of America.
3 Nanosciences African Network iThemba LABS-National Research Foundation, South Africa.
4 UNESCO-UNISA Africa Chair in Nanosciences/Nanotechnology, College of Graduate Studies, University of South Africa.
5 Africa Centre of Excellence for Sustainable Power and Energy Development, University of Nigeria.

UNISA
Nano-Horizons
https://unisapressjournals.co.za/index.php/NH
Volume 2 | 2023 | 14 pages

Nano-Horizons
https://doi.org/10.25159/3005-2602/13831
ISSN 3005-2602 (Online)

1 Introduction

Zinc oxide (ZnO) is an n-type inorganic wide band gap semiconductor that is thermally conductive with a direct energy band gap of about 3.4 eV, increased refractive index and ultraviolet shielding property [1], [2]. ZnO is useful in transparent electrode and electronic devices, anticorrosive coatings, lithium-ion batteries, thermal-protecting windows, transistors, and light-emitting diodes. The oxygen vacancies and zinc interstitials create room for successful doping of ZnO nanostructures [3]. Several elements such as copper, gallium, manganese, molybdenum (Mo), tin, boron and aluminium have been successfully used in doping ZnO nanomaterials [4], [5]. Doping is an effective way of manipulating the conductance of a semiconductor by utilising the characteristics of the dopant [6], [7]. It also helps to modulate the structure, light and electrical features of the semiconductor by altering the material's charge carrier concentration. Mo serves as an efficient dopant as it improves the thermoelectric features, enhances the carrier density, and has the tendency of increasing the band gap in the host material. The resistivity of ZnO can be reduced by introducing Mo to donate two or four conduction electrons [3]. Mo-doped ZnO nanomaterials are useful in photoelectrochemical water splitting, photovoltaic devices, transistor biosensors, and photocatalytic devices [3], [8]–[11].

Surfactants are useful in decreasing the surface tension and increasing stability at the interface [12]. Their amphiphilic feature is essential in preventing aggregation of the prepared nanomaterial and maintaining stability in the colloidal system. Understanding their mechanism and function in the synthesis process is useful in determining the performance and morphology of the prepared nanomaterial. Sodium dodecyl sulfate (SDS) has been reported to be a useful surfactant in improving surface modification, enhancing electrochemical performance, corrosion modulation, improving stability and thermal conduction [12]–[15]. Several techniques such as chemical vapour deposition, chemical bath deposition, hydrothermal, spin coating, sol-gel, and atomic layer deposition [1], [4], [5], [16], [17] have been adopted in preparing ZnO materials. Hydrothermal synthesis is a useful method for crystallising materials from thermally aqueous solutions at high vapour pressures, creating high quality nanoparticles and producing crystalline phases which are not stable at increasing temperatures with good control over the material composition [16].

Ramimoghadam *et al*. [18] studied the influence of SDS on the surface micrographs and structure of ZnO nanostructure. They obtained enhanced modifications in their shape and size. Aydin *et al*. [19] also investigated the impact of SDS-surfactant on the morphology and microstructure of copper oxide (CuO) nanomaterials. Most studies have focused on synthesising ZnO nanostructures via diverse techniques. In the absence of any surfactant, Zandsalimi *et al*. [11] synthesised Mo-doped ZnO nanoparticles at varying pH concentrations. Increasing the dopant concentration was reported to enhance the efficiency of the films and produced hexagonal-shaped nanoparticles. ZnO samples doped with Mo were prepared at varying concentrations of the dopant with polyethylene

glycol as the surfactant [20]. They obtained an amorphous structure with least transmittance recorded for the sample doped with the highest amount of Mo.

In this article, we focused on doping ZnO with Mo at varying concentrations. The effect of preparing SDS surfactant-assisted ZnO films during the synthesis process has also been investigated. However, insufficient investigations have been conducted on the influence of SDS surfactant on the features of ZnO doped at varying Mo concentrations of 0.3 M and 0.5 M.

2 Experimentals

2.1 Chemicals

All the reagents such as zinc nitrate hexahydrate ($Zn(NO_3)_2.6H_2O$), distilled water (H_2O), hexamethylenetetramine ($C_6H_{12}N_4$), molybdenum ($(NH_4)_6Mo_7O_{24}$) and SDS were of analytical grade (about 99.5% purity) and used without further purification.

2.2 Synthesis Process

Before deposition, the stainless steel and glass substrates were purified in a soapy solution, ultrasonicated in acetone for an hour, and further sterilised in an oven at 333 K for 24 hours. The synthesis process began by mixing 0.2 M of hexa-methylene tetramine solution, 0.8 M of zinc nitrate solution, and 0.25 M of SDS in a conical flask. Stirring was done in an ambient environment for about an hour to improve homogeneity. SDS was used as the surfactant to control the nucleation rate and rate of agglomeration [21]. A total of 0 M, 0.3 M and 0.5 M of ammonium heptamolybdate were used in doping the as-prepared solution after ultrasonicating for 20 minutes and stirring for 1 hour as shown in Figure 1. The solution was moved into an autoclave and oven heated at 90 °C for 4 hours to allow for a complete transformation from the hydroxide to the oxide phase of zinc [1]. The resulting ZnO films were then rinsed, cooled at room temperature and annealed at 400 °C for 1 hour to minimise unwanted surface roughness [22].

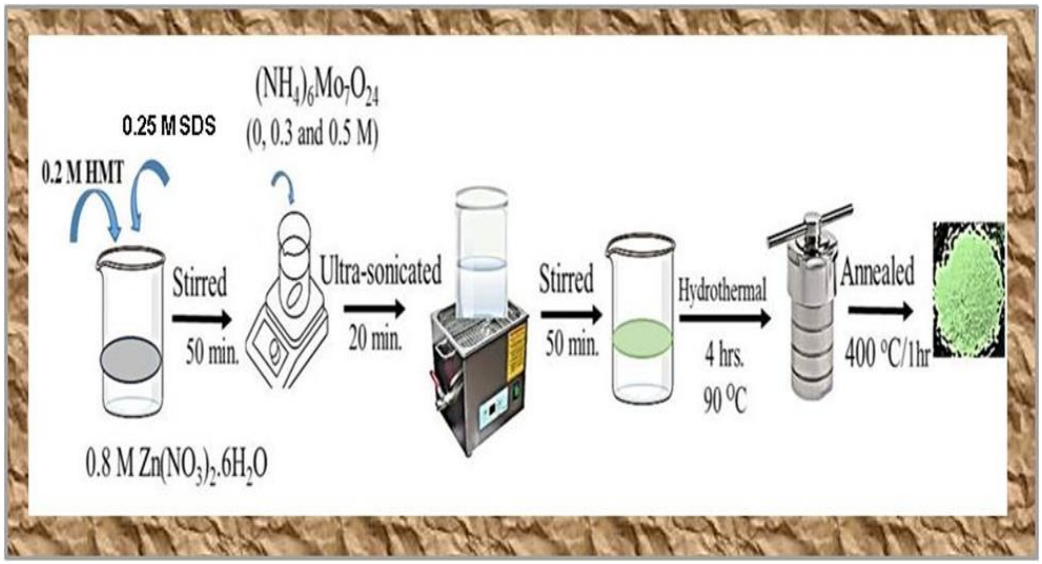

Figure 1: Stages in the preparation of the ZnO films using SDS as surfactant

2.3 Characterisations

To understand the behaviour of nanomaterials, the structural analysis was done using an X-ray diffractometer (XRD) (Rigaku D/MAX 2400, λ¼ 0.1544 nm). The XRD was useful in determining the crystal structure. The morphological make-up of the as-synthesised samples was characterised by using a scanning electron microscopy (SEM) (Nova Nano-SEM 450, 20 kV) and transmission electron microscopy (TEM) (Tecnai G2 F20 S-Twin, 200 kV). The chemical constituents of the synthesised nanomaterials were examined by energy dispersive X-ray spectroscopy (EDX) (AMETEK). An ultraviolet-visible (UV-Vis) spectrophotometer (756S UV-VIS) was used to investigate all optical properties of the samples.

3 Results and Discussion

3.1 XRD Analysis

The structural patterns of the undoped and Mo-doped ZnO samples are shown in Figure 2(a). The structure shows a hexagonal wurtzite crystalline phase with the most obvious peak seen at (1 0 0) plane for a 2theta value of 31.16° and with JCPDS number: 36-1451. Other diffraction peaks were obtained at orientation planes of (0 0 2), (1 0 1), (1 0 2) and (1 1 0) and correspond to 2theta values of 34.04°, 36.18°, 46.54°, and 55.56°. It is obvious that introducing SDS and adding more dopant significantly improved the crystallinity of the film as evident from the peak intensity, especially at the preferred plane. A slight observable shift for the most prominent peaks of the samples can be observed towards greater 2theta values as an indication of successful substitution of the

Mo for Zn in the lattice. Similar index patterns have also been reported in the literature [11].

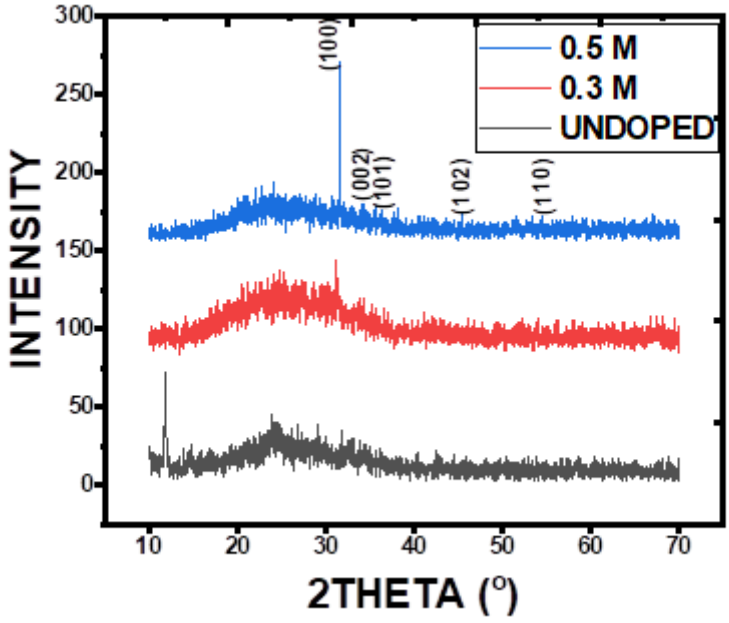

Figure 2(a): X-ray diffraction plots of the as-synthesised ZnO samples

The crystallite sizes of the undoped and doped samples were calculated using Debye Scherer's formula [23]. Other structural parameters such as the lattice constants (a and c) and the lattice strain (ε) have also been determined and are listed in Table 1. The lattice strain could be attributed to the dopant introduced at the lattice sites of the host material and the different ionic radii of zinc and Mo [10]. As the crystallite size increases, the lattice constants decrease towards increasing 2theta values.

TABLE 1. Structural parameters of the prepared ZnO nanomaterials

hkl	2θ (o)	FWHM (o)	D (nm)	a (nm)	c (nm)	ε
(1 0 0)	31.16	0.2196	65.52	0.3315	0.5741	0.1969
(0 0 2)	34.06	0.2189	66.22	0.3039	0.5265	0.1787
(1 0 1)	36.18	0.2160	67.50	0.2867	0.4966	0.1653
(1 0 2)	46.54	0.2144	70.37	0.2253	0.3903	0.1246
(1 1 0)	55.56	0.2137	73.31	0.1910	0.3308	0.1014

To further confirm the orientation planes of the synthesised samples, scanning area electron diffraction (SAED) was done as displayed in Figure 2(b). The SAED patterns correspond to the Miller indices (hkl) of the diffraction planes obtained from the X-ray diffractograms. The bright rings are an indication of the crystallinity of the prepared material.

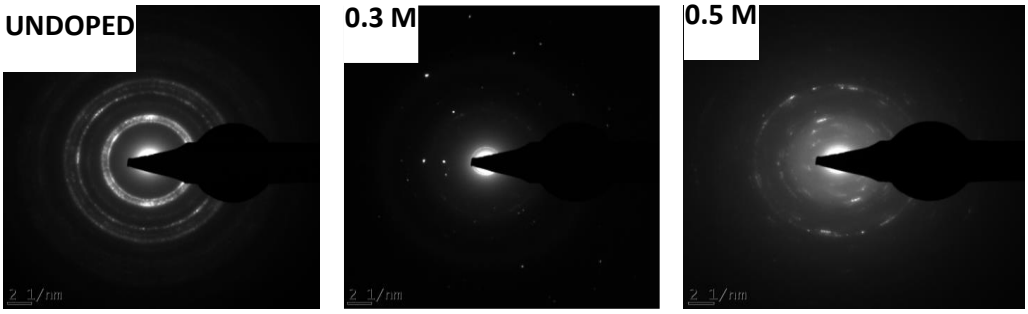

Figure 2(b): SAED images of the as-synthesised ZnO materials

3.2 Surface Morphologies

The surface morphologies were determined through the studies of scanning and transmission electron microscopy for the SDS-assisted Mo-doped ZnO thin films prepared at 0 M, 0.3 and 0.5 M concentrations of Mo. SDS played a role in identifying the film morphology that would produce the most efficient solar cell. The SEM micrograph for the undoped film shows a sticky micrograph owing to the optimisation technique adopted (Figure 3(a)). Introducing the dopant led to the elimination of the sticky surface morphology and resulted in long nanorods evenly distributed over the substrate surface. The nanorods obtained have been attributed to the inclusion of Mo as dopant [10]. Increasing the amount of Mo from 0.3 M to 0.5 M led to more agglomerations as seen in Figure 3(b). This could be due to the increased adhesion of dopant particles to each other as the Mo concentration got increased.

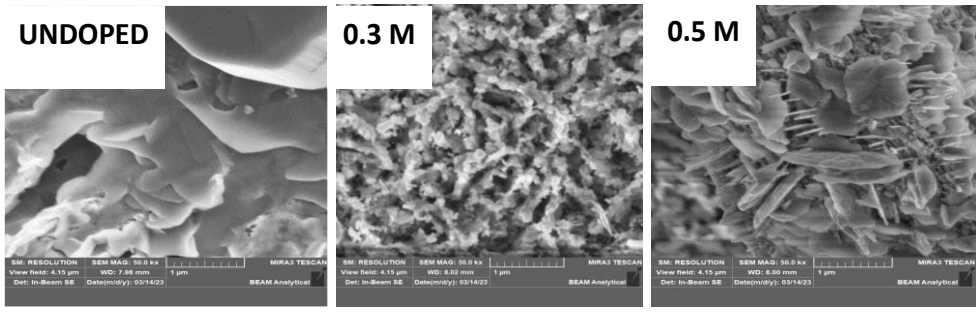

Figure 3(a): SEM images for the as-deposited ZnO nanomaterials

To further understand the material morphology as the electrons are transmitted, TEM images were taken as shown in Figure 3(b). The growth of the films can be visualised as tiny nanoclusters spreading through the material and nucleating to form larger lumps as the dopant concentration was increased. A further increase in the amount of dopant added led to a balloon-like morphology, owing to a combination of more clustered nanocrystals.

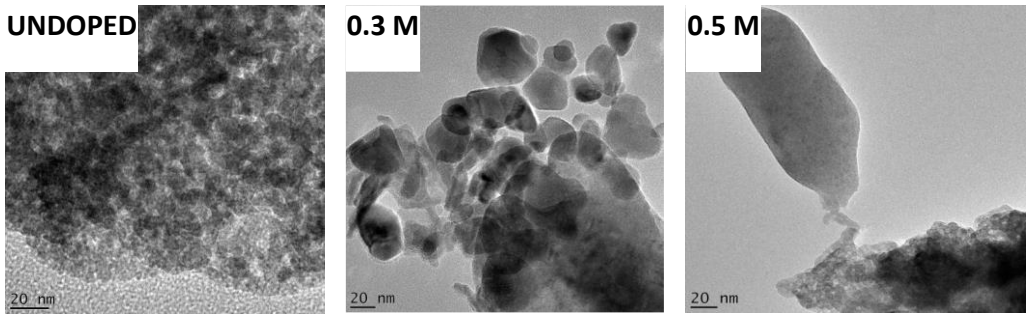

Figure 3(b): Transmission electron micrographs for the as-synthesised ZnO samples

3.3 Elemental Composition

The elemental constituents of the deposited materials are displayed in Figure 4. The plots confirm higher weight percentages of basic elements such as zinc and oxygen for the undoped samples. The doping process was confirmed as the doped samples revealed Mo as an additional element. The weight percentages have been tabulated and placed as insets in the plots. Variations in the basic elemental percentages could be due to the introduction of Mo as a dopant. The additional elements could be attributed to the substrate used and other external factors.

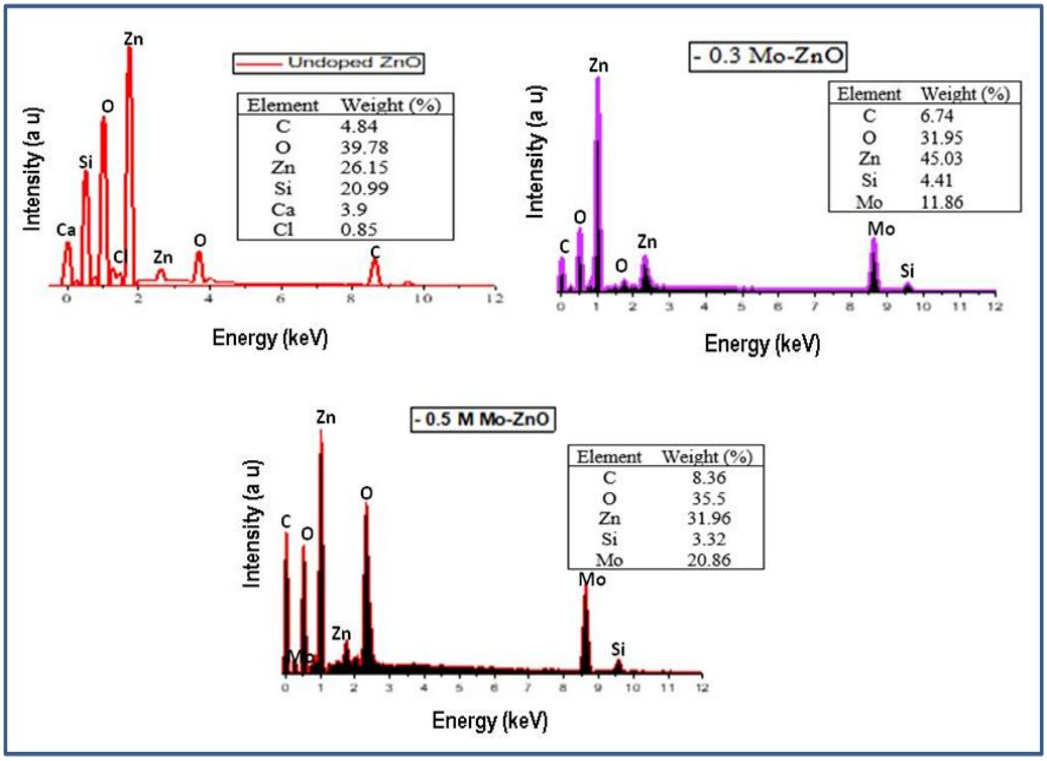

Figure 4: EDX plots of the ZnO films with insets of their weight percentages

3.4 Optical Characteristics

Plots of the absorbance and reflectance for the ZnO materials have been displayed in Figure 5. Maximum absorbance of over 70% was obtained for the ZnO material doped with 0.5 M of Mo. The addition of more dopant concentration yielded a reasonable increase in the absorbance of the film whereas the undoped film recorded the least absorbance as seen in Figure 5(a). This could be due to an increasing film thickness as more Mo is added to the solution. Similar results have been reported [3]. The highest doped film recorded the least reflectance percentage in the ultraviolet region, which increased towards increasing wavelength regions. Towards higher wavelength regions, the 0.3 M film recorded the least reflectance. An average reflectance of about 20% was recorded throughout the wavelength regions. The high absorbance nature of the doped samples could be responsible for the least reflectance observed and is a good trend for solar cell materials.

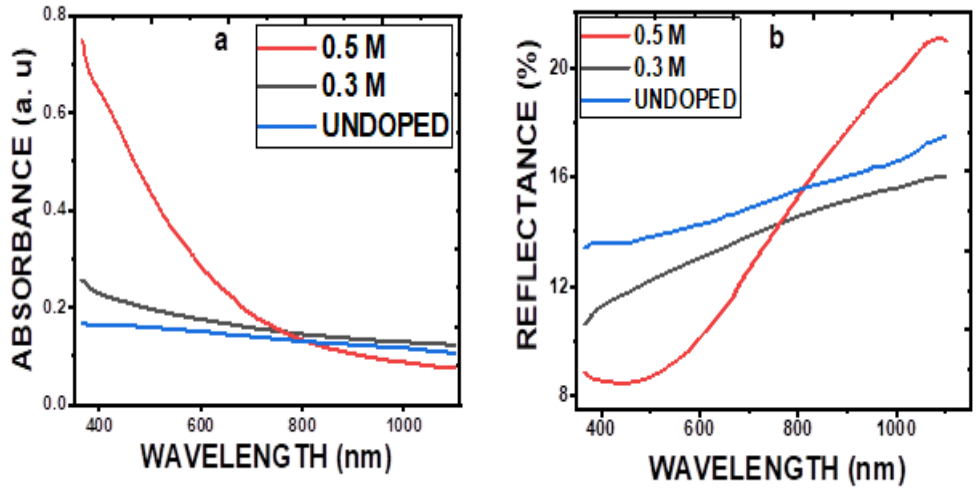

Figure 5: Optical plots showing the **(a)** absorbance and **(b)** reflectance of the deposited films

Figure 6(a) gives the absorption coefficient plots and shows varying trends at different electromagnetic spectra. In the ultraviolet and visible electromagnetic regions, the undoped film had the least absorption coefficient while the more doped ZnO film recorded increasing values towards decreasing wavelength regions. This feature accounts for their potential use in solar cells as they readily absorb photons in the visible spectrum. As the wavelength increases, the 0.5 M doped film displayed the least absorption coefficient. The energy band gap values seen in Figure 6(b) for the undoped, 0.3 M and 0.5 M are 3.70 eV, 3.84 eV and 3.97 eV, respectively. The high energy band gaps are due to the wide band gap nature of the ZnO semiconducting material. It can be observed that increasing the dopant concentrations due to the introduction of Mo led to decreasing band gap energy values of the samples. Similar band gap energies have been reported [1], [3]. The prepared films are useful in solar cells and electronic devices.

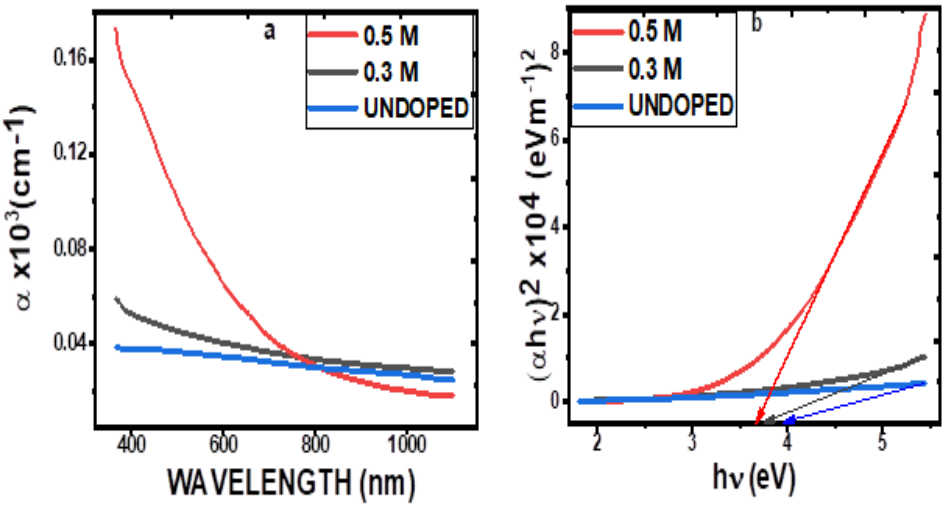

Figure 6: (a) Absorption coefficient and **(b)** energy band gap plots of the undoped and Mo-doped ZnO films

4 Conclusion

The effect of adding SDS as a surfactant in the preparation of ZnO nanomaterials was investigated. The effect of introducing 0.3 M and 0.5 M of Mo has also been discussed. The structure, morphology, and elemental and optical features of the films have also been studied. XRD and SAED patterns confirmed the wurtzite crystalline structure of the Mo-doped and undoped ZnO materials with the most prominent peak observed in the (1 0 0) orientation plane. SEM and TEM images revealed nanorods spread over the substrate surface at higher dopant concentrations. EDX confirmed the presence of as-deposited elements: Mo, Zn and O. Optical characterisations recorded increasing absorbance and decreasing reflectance values as more Mo was introduced. The energy band gap values for the undoped, 0.3 M, and 0.5 M films were 3.70 eV, 3.84 eV and 3.97 eV, respectively. The synthesised materials are useful in solar cell and optoelectronic devices.

References

[1] O. O. Apeh *et al*., “Properties of nanostructured ZnO thin films synthesized using a modified aqueous chemical growth method," *Mater. Res. Express*, vol. 6, no. 5, p. 056406, 2019, doi: 10.1088/2053-1591/aadcd6.

[2] A. C. Nkele, S. Ezugwu, M. Suguyima and F. I. Ezema, “Structural and electronic properties of metal oxides and their applications in solar cells,” in *Chemically Deposited Nanocrystalline Metal Oxide Thin Films: Synthesis, Characterizations, and Applications*. F. I. Ezema, C. D. Lokhande and R. Jose, Eds., Cham: Springer, 2021, pp. 147–163, doi: 10.1007/978-3-030-68462-4_6.

[3] D. Zhao, S. Sathasivam, J. Li and C. J. Carmalt, “Transparent and conductive molybdenum-doped ZnO thin films via chemical vapor deposition,” *ACS Appl. Electron. Mater.*, vol. 2, no. 1, pp. 120–125, 2019, https://doi.org/10.1021/acsaelm.9b00647.

[4] E. Benrezgua *et al*., “Synthesis and properties of copper doped zinc oxide thin films by sol-gel, spin coating and dipping: A characterization review,” *J. Mol. Struct.*, vol. 1267, p. 133639, 2022, doi: 10.1016/j.molstruc.2022.133639.

[5] S. D. Ponja, S. Sathasivam, I. P. Parkin and C. J. Carmalt, “Highly conductive and transparent gallium doped zinc oxide thin films via chemical vapor deposition,” *Sci. Rep.*, vol. 10, no. 1, p. 638, 2020, doi: 10.1038/s41598-020-57532-7.

[6] A. C. Nkele *et al*., “Role of metallic dopants on the properties of copper (1) iodide nanopod-like structures,” *Vacuum*, vol. 161, pp. 306–313, 2019, doi: 10.1016/j.vacuum.2018.12.049.

[7] R. O. Ijeh *et al*., “Optical, electrical and magnetic properties of copper doped electrodeposited MoO_3 thin films,” *Ceram. Int.*, vol. 46, no. 8, Part A, pp. 10820–10828, 2020, doi: 10.1016/j.ceramint.2020.01.093.

[8] S. D. Ghadge, M. K. Datta, O. I. Velikokhatnyi and P. N. Kumta, “Molybdenum doped bilayer photoanode nanotubes for enhanced photoelectrochemical water splitting,” *Int. J. Hydrog. Energy*, vol. 47, no. 2, pp. 993–1005, 2022, doi: 10.1016/j.ijhydene.2021.10.085.

[9] A. Kiruthiga and T. Krishnakumar, “Investigation of structural and magnetic properties of molybdenum doped ZnO nanostructures prepared by microwave-assisted wet chemical method,” *J. Ovonic Res*., vol. 15, no. 2, 2019.

[10] S. Nandanwar, M. W. Lee, S. Borkar, J. H. Cho, N. H. Tarte and H. J. Kim, “Synthesis, characterization, and anti-algal activity of molybdenum-doped metal oxides,” *Catal.*, vol. 10, no. 7, p. 805, 2020, doi: 10.3390/catal10070805.

[11] Y. Zandsalimi, R. Rezaee, E. Ghahramani and M. Moradi, “Photocatalytic efficiency of molybdenum-doped zinc oxide nanoparticles in treating landfill leachate,” *J. Adv. Environ. Health Res.*, vol. 7, no. 1, pp. 25–31, 2019.

[12] S. Deepa, B. K. Swamy and K. V. Pai, "A surfactant SDS modified carbon paste electrode as an enhanced and effective electrochemical sensor for the determination of doxorubicin and dacarbazine its applications: A voltammetric study," *J. Electroanal. Chem.*, vol. 879, p. 114748, 2020, doi: 10.1016/j.jelechem.2020.114748.

[13] M. Koundal, A. K. Singh and C. Sharma, "Study on the effect of imidazolium ionic liquid as a modulator of corrosion inhibition of anionic surfactant sodium dodecyl sulfate (SDS) on mild steel in sodium chloride solution," *J. Mol. Liq.*, vol. 350, p. 118561, 2022, doi: 10.1016/j.molliq.2022.118561.

[14] H. I. Elsaeedy, "A low temperature synthesis of Ag_2S nanostructures and their structural, morphological, optical, dielectric and electrical studies: An effect of SDS surfactant concentration," *Mater. Sci. Semicond. Process.*, vol. 93, pp. 360–365, 2019, doi: 10.1016/j.mssp.2019.01.022.

[15] A. I. Khan, "Experimental investigation of thermal conductivity and stability of TiO_2-Ag/water nanocompositefluid with SDBS and SDS surfactants," *Thermochim. Acta*, vol. 678, p. 178308, 2019, doi: 10.1016/j.tca.2019.178308.

[16] S. Mohan, M. Vellakkat, A. Aravind and U. Reka, "Hydrothermal synthesis and characterization of zinc oxide nanoparticles of various shapes under different reaction conditions," *Nano Express*, vol. 1, no. 3, p. 030028, 2020, doi: 10.1088/2632-959X/abc813.

[17] J. Panigrahi, P. K. Singh and G. Gupta, "Growth and luminescence characteristics of zinc oxide thin films deposited by ALD technique," *J. Lumin.*, vol. 233, p. 117797, 2021, doi: 10.1016/j.jlumin.2020.117797.

[18] D. Ramimoghadam, M. Z. B. Hussein and Y. H. Taufiq-Yap, "The effect of sodium dodecyl sulfate (SDS) and cetyltrimethylammonium bromide (CTAB) on the properties of ZnO synthesized by hydrothermal method," *Int. J. Mol. Sci.*, vol. 13, no. 10, 2012, doi: 10.3390/ijms131013275.

[19] R. Aydin and H. Cavusoglu, "Influence of sodium dodecyl sulfate as a surfactant on the microstructural, morphological and optoelectronic characteristics of SILAR deposited CuO thin films," *Mater. Res. Express*, vol. 6, no. 8, p. 086403, 2019, doi: 10.1088/2053-1591/ab1a08.

[20] D. C. Okeudo *et al*., "Influence of polyethylene glycol (PEG) surfactant on the properties of molybdenum-doped zinc oxide films," *J. Nano Mater. Sci. Res.*, vol. 2, no. 1, 2023, http://journals.nanotechunn.com/index.php/jnmsr/article/view/11.

[21] M. Vadivel, R. Ramesh Babu, M. Arivanandhan, K. Ramamurthi and Y. Hayakawa, "Role of SDS surfactant concentrations on the structural, morphological, dielectric and magnetic properties of $CoFe_2O_4$ nanoparticles," *RSC Adv.*, vol. 5, no. 34, pp. 27060–27068, 2015, doi: 10.1039/C5RA01162K.

[22] A. C. Nkele *et al*., "Structural, optical and electrochemical properties of SILAR-deposited zirconium-doped cadmium oxide thin films," *Mater. Res. Express*, vol. 6, no. 9, p. 096439, 2019, doi: 10.1088/2053-1591/ab31f5.

[23] A. C. Nkele *et al*., "Investigating the properties of nano nest-like nickel oxide and the NiO/Perovskite for potential application as a hole transport material," *Adv. Nat. Sci: Nanosci. Nanotechnol*., vol. 10, no. 4, p. 045009, 2019, doi: 10.1088/2043-6254/ab5102.